

Optical birefringence and polarization dependent loss of square- and rectangular-lattice holey fibers with elliptical air holes: numerical analysis

Y.C. Liu and Y. Lai

*Department of Photonics and Institute of Electro-Optical Engineering
National Chiao-Tung University, Hsinchu, Taiwan
ycl.eo91g@nctu.edu.tw, yclai@mail.nctu.edu.tw*

Abstract: Polarization dependent leakage loss as well as optical birefringence for the fundamental mode in square- and rectangular-lattice holey fibers with elliptical air holes are studied numerically based on the full-vector finite element method for the first time. It is shown that high birefringence in the order of 10^{-2} and large polarization dependent loss required for single-polarization single-mode transmission are both achievable by using the proposed structure.

©2005 Optical Society of America

OCIS codes: (060.2270) Fiber Characterization; (060.2280) Fiber design and fabrication; (060.2420) Fibers, polarization-maintaining; (060.2430) Fibers, single-mode

References and links

1. I. K. Hwang, Y. H. Lee, K. Oh and D. N. Payne, "High birefringence in elliptical hollow optical fiber," *Opt. Express* **12**, 1916 (2004), <http://www.opticsexpress.org/abstract.cfm?URI=OPEX-12-9-1916>.
2. T. P. Hansen, J. Broeng, S. E. B. Libori, E. Knudsen, A. Bjarklev, J. R. Jensen and H. Simonsen, "Highly birefringent index-guiding photonic crystal fibers," *IEEE Photon. Technol. Lett.* **13**, 588 (2001).
3. C. Kerbage, P. Steinvurzel, P. Reyes, P. S. Westbrook, R. S. Windeler, A. Hale and B. J. Eggleton, "Highly tunable birefringence microstructured optical fiber," *Opt. Lett.* **27**, 842 (2002).
4. A. Ortigosa-Blanch, J. C. Knight, W. J. Wadsworth, J. Arriaga, B. J. Mangan, T. A. Birks and P. St. J. Russell, "Highly Birefringent Photonic Crystal Fibers," *Opt. Lett.* **25**, 1325 (2000).
5. X. Chen, M. J. Li, N. Venkataraman, M. T. Gallagher, W. A. Wood, A. M. Crowley, J. Carberry, L. A. Zenteno and K. W. Koch, "Highly birefringent hollow-core photonic bandgap fiber," *Opt. Express* **12**, 3888 (2004), <http://www.opticsexpress.org/abstract.cfm?URI=OPEX-12-16-3888>.
6. A. H. Bouk, A. Cucinotta, F. Poli and S. Selleri, "Dispersion properties of square-lattice photonic crystal fibers," *Opt. Express* **12**, 941 (2004), <http://www.opticsexpress.org/abstract.cfm?URI=OPEX-12-5-941>.
7. P. St. J. Russell, E. Marin, A. Díez, S. Guenneau and A. B. Movchan, "Sonic bandgaps in PCF performs: enhancing the interaction of sound and light," *Opt. Express* **11**, 2555 (2003), <http://www.opticsexpress.org/abstract.cfm?URI=OPEX-11-20-2555>.
8. M. Y. Chen and R. J. Yu, "Polarization properties of elliptical-hole rectangular lattice photonic crystal fibres," *J. Opt. A* **6**, 512 (2004).
9. M. J. Steel and R. M. Osgood Jr., "Polarization and dispersive properties of elliptical-hole photonic crystal fibers," *J. Lightwave Technol.* **19**, 495 (2001).
10. M. J. Steel and R. M. Osgood Jr., "Elliptical-hole photonic crystal fibers," *Opt. Lett.* **26**, 229 (2001).
11. K. Saitoh and M. Koshiba, "Chromatic dispersion control in photonic crystal fibers: application to ultra-flattened dispersion," *Opt. Express* **11**, 843 (2003), <http://www.opticsexpress.org/abstract.cfm?URI=OPEX-11-8-843>.
12. K. Okamoto, "Single-polarization operation in highly birefringent optical fibers," *Appl. Opt.* **23**, 2638 (1984).
13. K. S. Chiang, "Stress-induced birefringence fibers designed for single-polarization single-mode operation," *J. Lightwave Technol.* **7**, 436 (1989).
14. J. R. Simpson, R. H. Stolen, F. M. Sears, W. Pleibel, J. B. Macchesney, and R. E. Howard, "A single-polarization fiber," *J. Lightwave Technol.* **1**, 370 (1983).

15. M. J. Messerly, J. R. Onstott, and R. C. Mikkelsen, "A broad-band single polarization optical fiber," *J. Lightwave Technol.* **9**, 817 (1991).
16. K. Saitoh, and M. Koshiba, "Single-polarization single-mode photonic crystal fibers," *IEEE Photon. Technol. Lett.* **15**, 1384 (2003).
17. H. Kubota, S. Kawanishi, S. Koyanagi, M. Tanaka, and S. Yamaguchi, "Absolutely single polarization photonic crystal fiber," *IEEE Photon. Technol. Lett.* **16**, 182 (2004).
18. D. Ferrarini, L. Vincetti, and M. Zoboli, "Leakage properties of photonic crystal fibers," *Opt. Express* **10**, 1314 (2002), <http://www.opticsexpress.org/abstract.cfm?URI=OPEX-10-23-1314>.
19. M. Koshiba and Y. Tsuji, "Curvilinear hybrid edge/nodal elements with triangular shape for guided-wave problems," *J. Lightwave Technol.* **18**, 737 (2000).
20. J. F. Lee, D. K. Sun and Z. J. Cendes, "Full wave analysis of dielectric waveguides using tangential vector finite elements," *IEEE Trans. Microwave Theory Technol.* **39**, 1262 (1991).
21. L. S. Andersen and J. L. Volakis, "Mixed order tangential vector finite elements for triangular elements," *IEEE Anten. Propag. Magz.* **40**, 104 (1998).
22. P. Falkenstein, C. D. Merritt, and B. L. Justus, "Fused preforms for the fabrication of photonic crystal fibers," *Opt. Lett.* **29**, 1858 (2004).

1. Introduction

It is well known that photonic crystal fibers (PCFs) or holey fibers (HFs) can offer more flexibility than conventional fibers in the design of optical fiber properties including the birefringence. According to the recent literature, high birefringence in PCFs can be produced by combining the asymmetric core and the large core-cladding index contrast [1], by introducing two-size air holes around the fiber core [2], and by selectively filling the air holes with polymer to obtain an asymmetric structure [3]. Up to date, the largest birefringence in experimental reports is $3.7 \cdot 10^{-3}$ for solid core (index guiding) HFs [4], and around 0.02 for photonic bandgap fibers [5]. Recently, the dispersion properties of square-lattice HFs with circular air holes have been studied numerically with the use of finite element method and compared with triangular-lattice HFs [6]. The experimental study of the sonic bandgap based on square-lattice PCF preforms has also been reported [7]. In the present study, we will investigate the optical properties of the fundamental mode in square-lattice and rectangular-lattice HFs with elliptical air holes based on the full-vector finite element method. One of our main goals is to find some suitable structure parameters that can be used for designing single polarization transmission fibers as well as high birefringence polarization maintaining fibers. For this purpose, optical properties of the fiber structures with different pitches (hole-to-hole spacing), air hole sizes and stress factors are calculated within the wavelengths ranging from 1.42 μm to 1.61 μm . We find that the birefringence can be increased to the order of 10^{-2} , which is larger than the reported experimental record with the order of 10^{-3} [4], by decreasing the pitch and the stress factor. The suggestion for achieving similar birefringence in the proposed structure has been reported based on the Finite-Difference-Time-Domain (FDTD) method [8], and in elliptical-hole triangular lattice PCFs based on the plane wave expansion [9, 10]. However, the confinement (or leakage) loss properties for these fiber structures have not been investigated yet since both methods are not efficient in the evaluation of the optical loss due to field leaking. In our studies, the full-vector Finite-Element-Method (FEM) accompanied with the anisotropic perfectly-matched-layers (PMLs) boundary condition [11] are adopted as an alternative approach to investigate both the birefringence and the leakage loss properties of the square- and rectangular-lattice holey fibers with elliptical air holes, by performing simulations for different fiber structure parameters.

One interesting finding from our simulation is that, for square-lattice structures, a small stress factor may introduce a large loss coefficient ratio between the two polarization states. Thus the square-lattice structures with small stress factors may be suitable for achieving the single polarization transmission, because the lights in the other polarization state will experience much larger leakage loss and disappear eventually. Here we have adopted the

approach of maintaining a large differential loss between the two fundamental polarization modes to achieve the single-polarization single-mode (SPSM) fibers [12, 13], in contrast to the other approach of making one of the polarization modes unguided [14, 15, 16, 17].

On the other hand, for achieving high birefringence with low polarization dependent loss, we find that the rectangular-lattice fibers may be more favorable. From the simulation, we observe that the birefringence is still large in the rectangular-lattice case with $\Lambda=2.32 \mu\text{m}$, $a=0.3$, $s=0.35$, and $\Lambda_x=0.2 \Lambda$, while the polarization dependent loss coefficient ratio becomes much smaller. Thus, by putting enough layers of the holes to make the leakage losses of both polarizations low enough [18], this fiber structure should be suitable to serve as high birefringence polarization maintaining fiber. In the following sections we shall provide the detailed simulation results on which the above statements are based.

2. Square-lattice fiber structure

The square-lattice fiber structure used in our simulation is depicted in Fig. 1. Here Λ is the hole-to-hole distance (or pitch) and the silica index is assumed to be 1.45. In all the calculation of this section, the number of the elliptical air hole layers is assumed to be 5 (i.e., five-ring elliptical air holes). The elliptical air holes can be specified by transforming the circular air holes with a specified stress factor s , which is defined as follow:

$$s = \frac{d_x}{d} = \frac{d}{d_y} \quad (1)$$

The relation between the ellipticity and the stress factor s is

$$e = \frac{d_x}{d_y} = s^2 \quad (2)$$

As shown in Fig. 2, d_x and d_y are the minor axis and major axis lengths of the elliptical air hole respectively and d stands for the diameter of the circular air hole. Moreover, the air hole size ratio parameter a is defined as

$$a = \frac{d}{\Lambda} \quad (3)$$

In our simulation, the full-vector FEM with hybrid edge/nodal element as well as the anisotropic perfectly-Matched-Layers (PMLs) boundary condition are applied to study the proposed five-ring-air-hole structure [19, 11]. Triangular mesh elements are generated to divide the solution domain and the waveguide symmetry is exploited to reduce the area size of the domain by a factor of 4 for saving the computational labors. Each triangular mesh element has three nodes in the middle of the edges and three nodes on the corners. The element model we use is based on the constant tangential/linear normal (CT/LN) vector basis functions with the three edge nodes for the transverse field interpolation and the linear basis functions with the three corner nodes for the axial field interpolation [19]. The CT/LN edge element is also known as the mixed-order tangential vector finite element (TVFE) of order 0.5, because it provides a constant tangential/linear normal field along the element edges and a linear field inside the element [20, 21]. After applying the full-vector finite element procedure, a complex generalized eigenvalue equation can be obtained. The eigenvalue equation is then solved by a modified Matlab function and the effective index n_{eff} of the fundamental mode can be obtained from the corresponding complex eigenvalue. The birefringence between the x and y polarized modes is determined by taking the real part of the effective index difference of the two polarization modes. Figure 3 and Fig. 4 show the birefringence for fibers with $a=0.6$ and $a=0.7$ respectively. We can learn that, for a fixed air hole size ratio, structures with smaller pitches

and stress factors exhibit higher birefringence. For the fixed pitch cases in Fig. 5 and Fig. 6, the birefringence is higher when the stress factor is smaller. This is because a smaller stress factor will cause the structure to be more nonsymmetrical, while a smaller pitch will lead a larger core-cladding index contrast. Hence, higher birefringence can be expected. Figure 7 shows the birefringence of the structures with $\Lambda=1.0\ \mu\text{m}$, $a=0.6$, $s=0.7$, and $\Lambda=1.0\ \mu\text{m}$, $a=0.6$, $s=0.64$ respectively. The birefringence is of the order of 10^{-2} , which is higher than the recent experimental record 10^{-3} [4]. When the stress factor s changes from 0.7 to 0.64, the birefringence raises significantly. The number of unknowns used in the simulation for this case is 156572 with $s=0.7$ and 133689 with $s=0.64$ (only one quarter of the fiber structure needed to be simulated due to symmetry). We have especially checked the numerical accuracy for the structure with $s=0.64$ and confirmed that the accuracy is better than 10^{-3} . The simulation is performed on a Pentium 2.0GHz personal computer equipped with 2.0GB RAM by using the Matlab software. Typically it will require 12hrs to obtain a birefringence (loss)-versus-wavelength curve from calculation.

Although we have seen that the birefringence can be increase to the order of 10^{-2} , the polarization dependent leakage loss still needs to be evaluated before one can conclude the fiber structures to be useful. The leakage loss can be determined according to the following formulation:

$$\text{Leakage loss} = \frac{2 \cdot 10^7}{\ln(10)} \cdot \frac{2\pi}{\lambda} \cdot \text{Im}[n_{\text{eff}}] \quad (\text{dB/m}) \quad (4)$$

As shown from Fig. 8 to Fig. 10, the loss difference between the x-polarized mode and the y-polarized mode increases for smaller stress factor when the pitch and the hole size are fixed. One can observe that the loss of y-polarized mode is greater than that of x-polarized mode. This is because a smaller stress factor makes the hole diameter become smaller in the x-direction and thus allow the y-polarized fields leaks more to the cladding than the x-polarized field does. Based on this observation, the square-lattice structures with elliptical holes may not be suitable for achieving high birefringence polarization maintaining due the large polarization dependent loss difference. However, they may be suitable for achieving the single-polarization single-mode transmission by taking the advantage of the large polarization dependent differential loss. For the structure shown in Fig. 11, at $1.55\ \mu\text{m}$, the loss coefficient ratio of the y-polarized mode compared to the x-polarized mode is about 76.7, and the leakage loss of the x-polarized mode can be made below 0.1dB/km. We have also confirmed that there is no higher order guided mode in this structure by making sure that there is no eigen-solution between the effective index of the fundamental mode and the fundamental space-filling mode (FSM) for both polarization states respectively. Hence, this structure should be suitable to achieve the single-polarization single-mode transmission. The magnitude of the loss coefficients for both polarizations can be engineered by adjusting the value of Λ . A smaller Λ will increase the loss coefficients for both polarizations, as can be seen from the comparison of Fig. 8 and Fig. 10. This may be desirable if one wants to reduce the required fiber length for achieving a given extinction ratio for different application purposes.

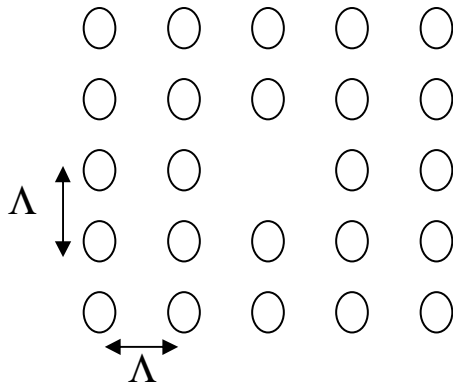


Fig. 1. The structure of the square-lattice HF with elliptical air holes.

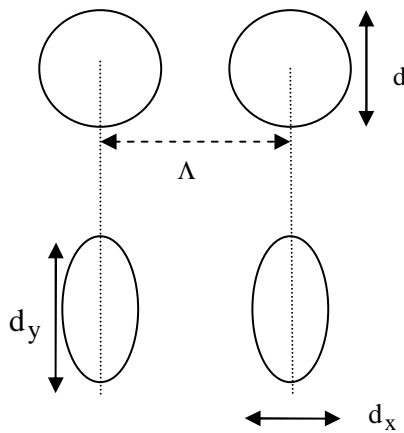


Fig. 2. Illustration of the structure parameters.

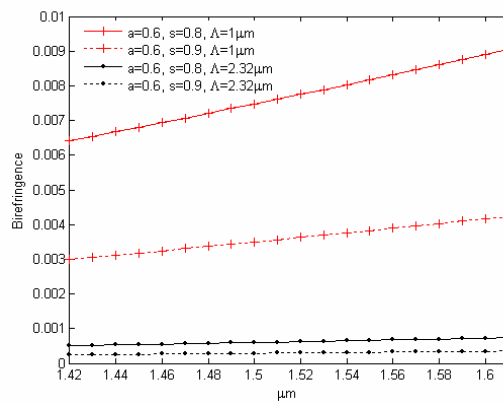


Fig. 3. The birefringence for the cases with $a=0.6$. The solid lines are with $s=0.8$ and the dot lines are with $s=0.9$.

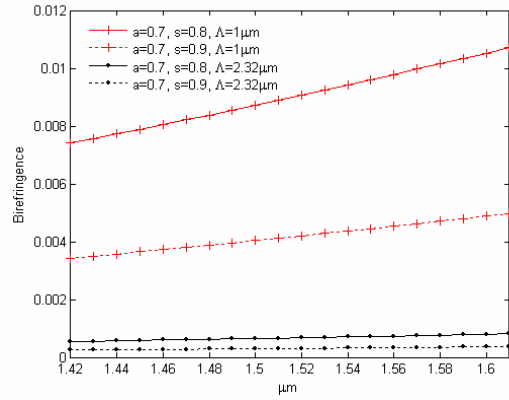


Fig. 4. The birefringence for the cases with $a=0.7$. The solid lines are with $s=0.8$ and the dot lines are with $s=0.9$.

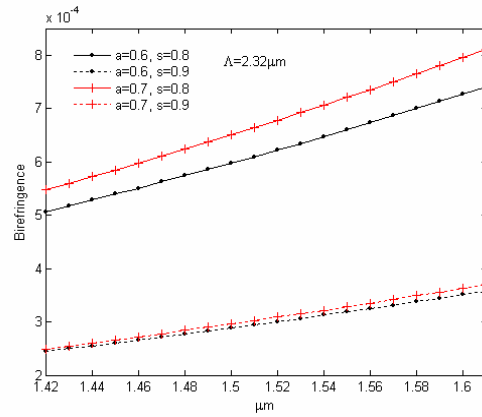


Fig. 5. The birefringence for the cases with $\Lambda=2.32 \mu\text{m}$. The solid lines are with $s=0.8$ and the dot lines are with $s=0.9$.

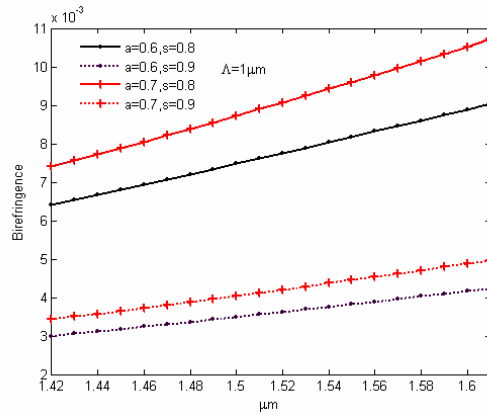


Fig. 6. The birefringence for the cases with $\Lambda=1 \mu\text{m}$. The solid lines are with $s=0.8$ and the dot lines are with $s=0.9$.

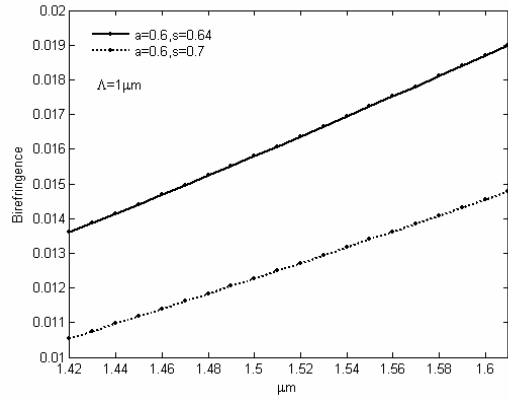


Fig. 7. The birefringence for the cases with $\Lambda=1 \mu\text{m}$, $a=0.6$.

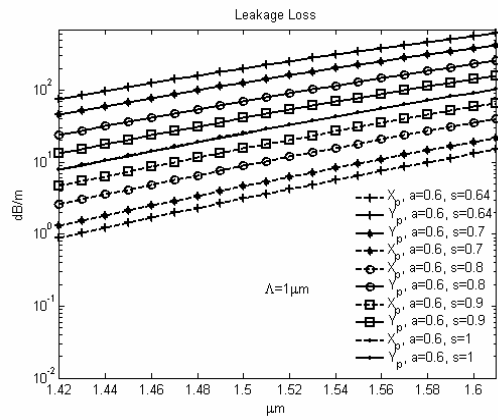


Fig. 8. The leakage loss for the cases with $\Lambda=1 \mu\text{m}$, $a=0.6$.

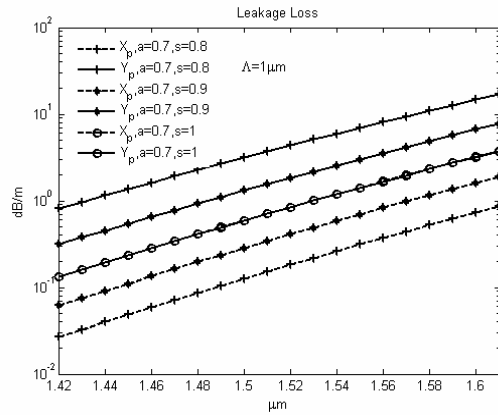


Fig. 9. The leakage loss for the cases with $\Lambda=1 \mu\text{m}$, $a=0.7$.

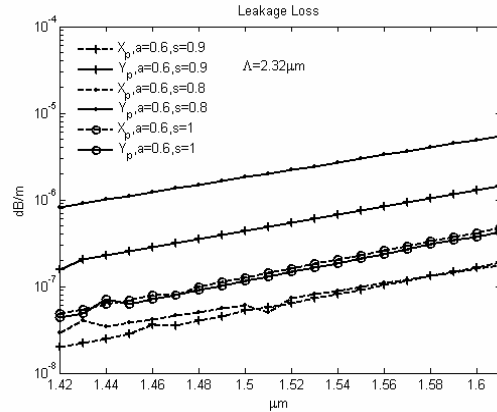


Fig. 10. The leakage loss for the cases with $\Lambda=2.32 \mu\text{m}$, $a=0.6$. The irregularities in the lower two curves should be due to the numerical inaccuracy when the imaginary part of the eigenvalue is too small and can be discarded.

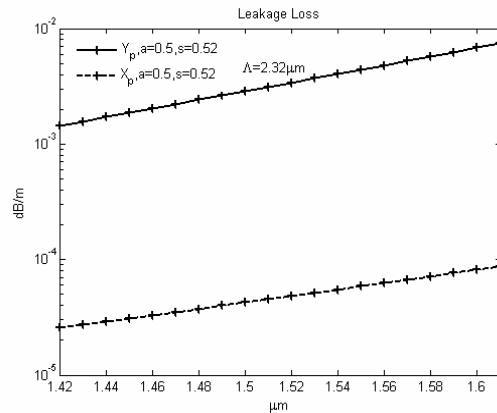


Fig. 11. The leakage loss for the cases with $\Lambda=2.32 \mu\text{m}$, $a=0.5$, and $s=0.52$.

3. Rectangular-lattice fiber structure

In order to reduce the polarization dependent loss ratio, we change the square-lattice structure into the rectangular-lattice arrangement and re-calculate the results. The structure in our simulation is shown in Fig. 12. Here Λ_x is the hole-to-hole distance (pitch) in the x-direction, and the parameter a , s , and Λ are fixed to 0.3, 0.35, and $2.32 \mu\text{m}$ respectively. The number of air holes in our simulation is the same as that depicted in Fig. 16. Two cases are considered in the simulation: (1) $\Lambda_x=0.4\Lambda$, (2) $\Lambda_x=0.2\Lambda$. From Fig. 13, one can observe that the birefringence is larger for $\Lambda_x=0.2\Lambda$ than for $\Lambda_x=0.4\Lambda$, because a smaller Λ_x makes the structure more asymmetric. The achieved birefringence here is somewhat larger than that in the square-lattice structure, but still in the order of 10^{-2} . Figure 14 and Fig. 15 show the leakage loss for the cases with $\Lambda_x=0.4\Lambda$ and $\Lambda_x=0.2\Lambda$ respectively. The loss ratio of the y-polarized mode to the x-polarized mode at $1.55 \mu\text{m}$ is about 0.53 for the case with $\Lambda_x=0.2\Lambda$, which is much smaller than the value of 25 for the case with $\Lambda_x=0.4\Lambda$. Based on this observation, the fiber structure with $\Lambda_x=0.2\Lambda$ exhibits the possibility of achieving the high birefringence polarization maintaining property with a small polarization dependent loss ratio. Here we simply try to minimize the loss coefficient “ratio” between the two polarizations by

using a fixed number of hole layers. Due to the thinner layers of holes, the results of the leakage loss in Fig. 15 tend to be high and the mode field patterns in Fig.16 seem to be not well confined. In practice this should not be a problem since it can be overcome easily by increasing the number of air hole layers [18]. The field patterns in Fig.16 are for $\Lambda_x=0.2\Lambda$ at $1.55 \mu\text{m}$. Compared to the y-polarized field, the x-polarized field is less confined in the core region. This also supports that the loss of the x-polarized field should be larger than that of the y-polarized field, as has been shown in Fig. 15. The number of unknowns in both cases are 141120 and 169229 respectively and the numerical accuracy has also been double checked. Again, only one quarter of the fiber structure is needed to be simulated due to the symmetry of the structures.

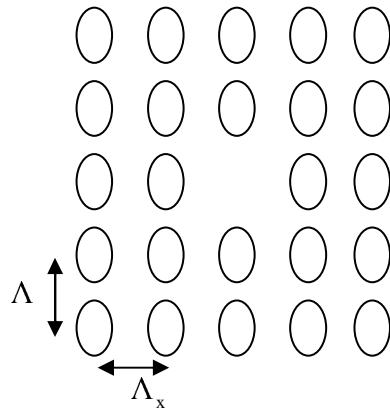


Fig. 12. The structure of rectangular-lattice HF with elliptical air holes.

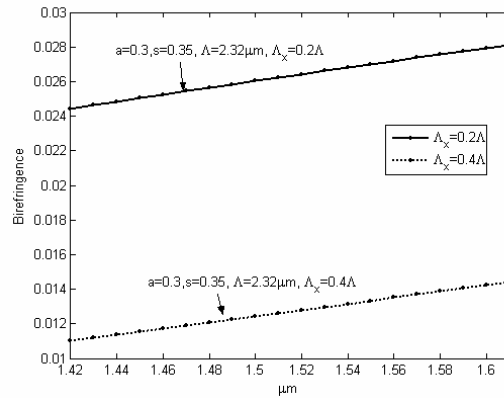


Fig. 13. The birefringence of rectangular-lattice HFs for $\Lambda_x=0.4\Lambda$ and $\Lambda_x=0.2\Lambda$ respectively.

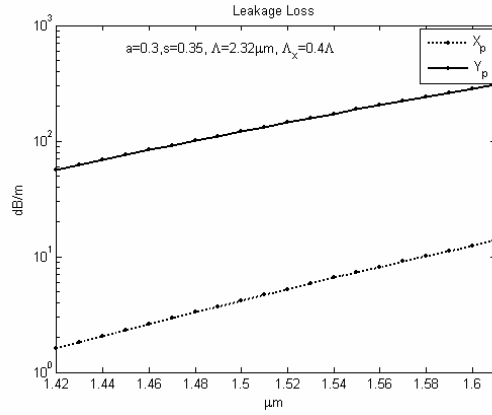


Fig. 14. The leakage loss of rectangular-lattice HFs for x-polarized mode and y-polarized mode respectively with $\Lambda_x=0.4\Lambda$.

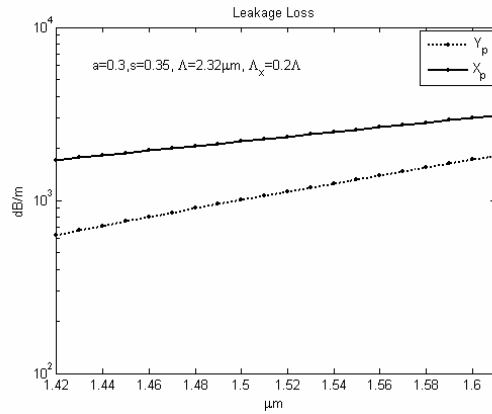


Fig. 15. The leakage loss of rectangular-lattice HFs for x-polarized mode and y-polarized mode respectively with $\Lambda_x=0.2\Lambda$.

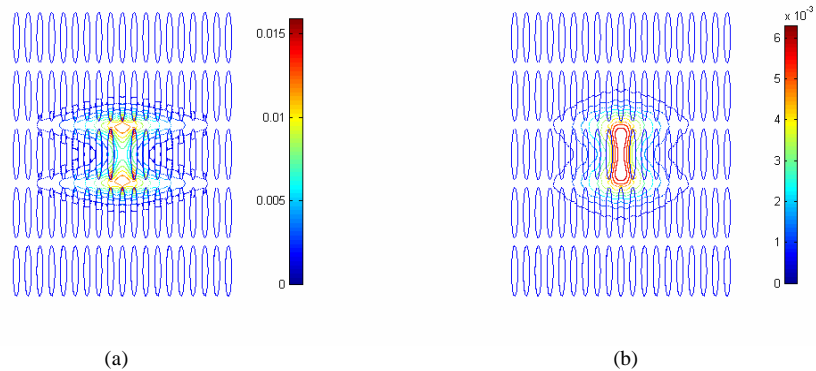


Fig. 16. Contour plots of the field magnitude for (a) E_x mode of the rectangular-lattice HF with $\Lambda_x=0.2\Lambda$ at $1.55\ \mu\text{m}$; (b) E_y mode of the rectangular-lattice HF with $\Lambda_x=0.2\Lambda$ at $1.55\ \mu\text{m}$. The increment between adjacent contours is $1/10$ of the peak value.

5. Conclusion and discussions

In this paper the influences of fiber structure parameters on the birefringence and the polarization-dependent leakage loss of the square- and rectangular-lattice holey fiber structures with elliptic air holes have been investigated in details. It has been shown that high birefringence to the order of 10^{-2} can be reached by decreasing the pitch and the stress factor. We have also found that, for square-lattice structures, a small stress factor introduces larger loss difference between the two polarization states. Thus the square-lattice structures with small stress factors may be more suitable for achieving the single polarization transmission. For achieving high birefringence with low polarization dependent loss, we find that the rectangular-lattice fibers should be more favorable, since their polarization-dependent loss ratio can be made much smaller by properly adjusting the hole distance in two directions. Based on these simulation results, we conclude that both the single polarization transmission and the high birefringence polarization maintaining can be achieved by using the proposed structures with suitable parameters respectively.

Even though the present study is purely theoretical, at the end of this paper we would like to briefly comment on the possible fabrication issues for the proposed fiber structure, although the only way to know the answer really is to try it. For current PCFs with small holes, typically there is considerable variation in precise hole size and shape. The holes may be particularly susceptible to changes in shape due to collapse and the surface tension may also tend to pull elliptic holes into circular ones. It seems that up to date one of the most promising fabrication methods that can overcome these problems may be the new multi-step process of forming preforms [22]. In this new method, compared to the conventional stacking procedure, the rods and tubes made of two different glass materials respectively are first stacked, then fused and finally etched to form the preform before being drawn. Since the fusing process is performed in advance, the drawing temperature can be kept as low as possible to minimize the shape distortion during the later drawing process. Even though right now only circular shapes are demonstrated with this method, hopefully in the future the method can be extended to fabricate elliptical holes with smaller hole distance and/or with large stretching.

Acknowledgments

One of the authors (Y.C. Liu) would like to thank Dr. Din-Kow Sun and Prof. Koshiha for their help on the numerical method of FEM.